Molecular Catalysis 528 (2022) 112496

Contents lists available at ScienceDirect

Molecular Catalysis

journal homepage: www.journals.elsevier.com/molecular-catalysis

A novel 4-hydroxyacetophenone monooxygenase featuring aromatic substrates preference for enantioselective access to sulfoxides

Shiyu Wei, Guochao Xu *, Jieyu Zhou, Ye Ni *

Key Laboratory of Industrial Biotechnology, Ministry of Education, School of Biotechnology, Jiangnan University, Wuxi, Jiangsu 214122, China

ARTICLE INFO

Keywords:
HAPMO
Substrate specificity
Enantioselectivity
Asymmetric sulfoxidation

ABSTRACT

Baeyer-Villiger monooxygenases are recognized as valuable tools for biooxidative synthesis of chiral sulfoxides. In this work, a novel HAPMO ortholog from *Pseudomonas fluorescens* ($HAPMO_{Pf}$) was identified by genome mining. Evolutionary relationship and sequence analysis revealed that $HAPMO_{Pf}$ belongs to the family of typical type I BVMOs. $HAPMO_{Pf}$ has a low K_M value (0.025 mM) toward 4-hydroxyacetophenone, and a half-life of 24 h at 30 °C and pH 9.0. $HAPMO_{Pf}$ exhibited distinct activity toward aromatic ketones as well as various thioethers, such as methyl phenyl sulfide and bromo-methyl phenyl sulfide. The highest activities of $HAPMO_{Pf}$ was 1.47 $U{\cdot}mg^{-1}$ toward 4-hydroxyacetophenone among tested ketone and thioether substrates. Furthermore, over 95% enantioselectivity was determined toward methyl phenyl sulfides with *ortho, meta,* and *para*-substituents (Cl, Br, CHO, NH_2). Therefore, $HAPMO_{Pf}$ is a promising biocatalyst for the synthesis of aromatic esters and chiral sulfoxides.

Introduction

Some bacteria degrade aromatic compounds such as acetophenone [1–3] and 4-ethylphenol [4] via enzyme-mediated Baeyer-Villiger reactions, in which an oxygen atom is inserted between the aromatic ring and the ketone side chain [5]. For example, *Pseudomonas fluorescens* ACB utilizes 4-hydroxyacetophenone as the sole carbon and energy source [1]. Baeyer-Villiger monooxygenases (BVMOs) are flavoenzymes capable of catalyzing Baeyer-Villiger reaction using oxygen and NAD(P)H [5]. Flavoprotein monooxygenasesn (FPMOs) are divided into six groups (Group A, B, C, D, E and F) according to their distinct structural and functional properties. Among them, group B FPMOs represent mainly Baeyer-Villiger monooxygenases (Type I BVMOs) and heteroatom oxygenases [6–8]. $HAPMO_{pf\ ACB}$ (4-hydroxyacetophenone monooxygenase), a type I Baeyer-Villiger monooxygenase (BVMO) that catalyzes NADPH-dependent oxidation of 4-hydroxyacetophenone to 4-hydroxyphenylacetate was identified from *Pseudomonas fluorescens* ACB and characterized [9]. $HAPMO_{pf\ ACB}$ is a homodimer of 145 kDa with each subunit containing a tightly and non-covalently bound FAD as cofactor [9], and represents the first reported BVMO exhibiting primary activity toward aromatic compounds. Rehdorf and coworkers reported the second HAPMO from *Pseudomonas putida* JD1($HAPMO_{pp}$), which is involved in the metabolism of 4-ethylphenol [10]. Thermostable BVMO from *Thermobifida fusca* (PAMO) identified by genome mining, is active toward a wide range of aromatic ketones, however with poor enantioselectivity for sulfoxidation reaction. So far, only three BVMOs, $HAPMO_{pf\ ACB}$ [9], $HAPMO_{pp}$ [10] and phenylacetone monooxygenase (PAMO) [11], capable of converting aliphatic and aromatic ketones, were described. However, most reported BVMOs are dedicated to convert cyclohexanone and related cyclic aliphatic ketones. There is an increasing demand to discover novel BVMOs with diverse biocatalytic properties.

Chiral sulfoxides have gained great attention as synthons and precursors for the synthesis of APIs (Active Pharmaceutical Ingredient) [12,13] flavors and fragrances [14] as well as chiral auxiliaries in chemical synthesis [15]. Chiral sulfoxides can be prepared by resolution of racemates, direct asymmetric oxidation of prochiral sulfides [16,17] by chemical [18] and biological catalysts with enantioselective advantages [19]. The biooxidation of prazole sulfides has been explored by several groups. For example, the oxidation of methyl phenyl sulfide by *Rhodococcus* sp. ECU0066 whole cells [20], AbIMO [21] and *pm*MsrA [22], where (*S*) and (*R*)-phenyl methyl sulfoxides were produced with high enantiomeric excesses (≥ 94% *ee*). Remarkably, HAPMO from *P. fluorescens* ACB has been reported to produce optically pure (*S*)-enantiomers (> 99% *ee*) toward phenyl methyl sulfide substituted with *para*-electron donating groups [23,24], which is regarded as an

* Corresponding authors.
E-mail addresses: guochaoxu@jiangnan.edu.cn (G. Xu), yni@jiangnan.edu.cn (Y. Ni).

https://doi.org/10.1016/j.mcat.2022.112496
Received 24 April 2022; Received in revised form 3 July 2022; Accepted 5 July 2022
Available online 20 July 2022

appropriate template for genome mining.

Although two HAPMOs from *P. fluorescens* ACB and *P. putida* JD1 have been identified, HAPMOs toolbox with versatile substrate specificity is far from sufficient. This study aims to explore novel 4-hydroxyacetophenone monooxygenases and their catalytic properties. Here, we identified a HAPMO ($HAPMO_{Pf}$) from *P. fluorescens* FW300-N2E2 and investigated its activity in enantioselective sulfoxidation reactions. This newly discovered $HAPMO_{Pf}$ enriches BVMOs library, and provides a potential biocatalyst for the synthesis of chiral sulfoxides.

Material and methods

Materials

All chemicals and reagents were from commercial sources and purchased from Sigma-Aldrich (Stockholm, Sweden), Aladdin (Beijing, China) and Macklin (Shanghai, China). All PCR reagents and enzymes were purchased from Takara (Dalian, China).

Genome data mining for HAPMOs

A library of putative Baeyer-Villiger monooxygenases was constructed by genome mining. A total of ten monooxygenases, varying between 30% and 90% sequence identity of $HAPMO_{pf\ ACB}$, were selected from the UniProt/Swiss-Prot database.

Sequence analysis of $HAPMO_{pf}$

Multiple sequence alignment was performed by MAFFT V.7 [25]. The phylogenetic tree was generated with MEGA-X using the Neighbor-joining method [26].

Plasmid construction, microbial strains and culture media

The optimized DNA fragment containing the selected $HAPMO_{Pf}$ gene from *Pseudomonas fluorescens* FW300-N2E2 (genomic DNA accessione: AMZ71204; protein accession: WP_063321766.1) was directly cloned into pET28a (+) between *Nde*I and *Bam*HI recognition sites, respectively. The sequence of the synthesized gene was confirmed by sequencing using T7 and T7term primers. *E. coli* strain BL21 (DE3) was chemically transformed with the plasmid by standard procedures [27], and monoclonal cells were grown at 37 °C in LB-agar medium (50 μg/mL kanamycin).

Enzyme overexpression and purification

$HAPMO_{Pf}$ encoding gene was expressed in *E. coli* BL21(DE3) using fresh LB medium containing 50 $\mu g \cdot mL^{-1}$ kanamycin. Cells were grown until optical density reached 0.6–0.8 when IPTG was added at a final concentration of 0.2 mM for induction at 16 °C for 20 h. The cells were then harvested by centrifugation at 4 °C and 10,000 × g for 10 min, washed twice with sterile Tris-HCl buffer (pH 9.0, 100 mM), and disrupted by ultra sonication (2 s working and 3 s resting for 10 min, 250 W). The lysate was centrifuged for 30 min at 10,000 × g and 4 °C. The supernatant was taken as crude extract, and was purified by Ni-NTA affinity chromatography at 4 °C using His-Trap Ni-nitrilotriacetic acid FF column (5 mL, GE Healthcare Bioscience). After 50−250 mM imidazole gradient elution from the column, fractions containing $HAPMO_{pf}$ activity were pooled and concentrated. The soluble expression and purity of $HAPMO_{Pf}$ was evaluated by SDS-PAGE.

Effects of temperature and pH

Influence of pH on activity of $HAPMO_{Pf}$ was evaluated at pH values ranging from 6.0 to 11.0, using sodium phosphate buffer (pH 6.0–9.0, 100 mM), Tris-HCl buffer (pH 8.5–9.5, 100 mM) and glycine-NaOH buffer (pH 9.5–11.0, 100 mM). Effect of temperature on activity of $HAPMO_{Pf}$ was measured by determining the relative activity toward 4-hydroxyacetophenone (S1) at temperature ranges of 20–50 °C in Tris-HCl buffer (pH 9.0, 100 mM). The thermal stability of purified $HAPMO_{Pf}$ was determined by examining the residual activity of preincubated enzyme solution at 30 and 40 °C for indicated periods of time. All activity assays were carried out in triplicate.

Effect of organic solvents on activity

Organic solvents (methanol, ethanol, isopropanol, acetone, acetonitrile, DMSO) on the solvent stability of HAPMO was explored in Tris-HCl buffer (pH 9.0, 100 mM) at 30 °C. Appropriate amount of purified $HAPMO_{Pf}$ was incubated with organic solvents (5%, v/v) for 2 h, and aliquots were taken to measure the residual activity using the standard assay. Control experiment with addition of equal volume of Tris-HCl buffer at same incubation time was regarded as 100%. All activity assays were carried out in triplicate.

Substrate specificity

Acetophenones with hydroxy group at *ortho, meta, para*-positions of the phenyl ring and six different *para*-substituted-acetophenones substrates (F-, Cl-, NH_2-, CH_3-, CH_3O-, NO_2-) were tested for determining the substrate specificity. Additionally, conversion and enantioselectivity of $HAPMO_{pf}$ toward methyl phenyl sulfide (S17) and methyl phenyl sulfide derivatives bearing electron-donating groups ($\sigma < 0$; OCH_3, NH_2) or electron-withdrawing groups ($\sigma > 0$; Cl, Br) at *ortho, meta, para*-positions of the phenyl ring were determined. Finally, some aliphatic ketones were measured, including cyclic ketones and open-chain ketones. The assays were carried out in standard conditions (100 mM Tris-HCl, pH 9.0, 30 °C). At different time intervals, samples were withdrawn and processed as above mentioned for chiral GC and HPLC analysis. All the measurements were performed in triplicate.

Kinetic measurements

Kinetic parameters were determined using the general activity assay protocol, S1, S6 (0.01–0.25 mM), S2, S3 (0.25–2.5 mM) and S4, S5, S7, S8 and S18 (0.1–10 mM) concentrations were used. All kinetic measurements were performed at 30 °C. The kinetic parameters were calculated according to non-linear curve fitting with Michaelis–Menten equation. All concentrations were measured in triplicate.

Homologous modeling and molecular docking analysis of $HAPMO_{Pf}$

We have used Rosetta (https://robetta.bakerlab.org/submit.php) structure prediction to predict the three-dimensional structure of $HAPMO_{Pf}$. The modeling method is RoseTTAFold. The structural model of $HAPMO_{Pf}$ was evaluated by SAVES v6.0 (https://saves.mbi.ucla.edu). Molecular docking analysis was performed by Discovery studio 4.5.

Sulfoxidation catalyzed by $HAPMO_{pf}$ in whole-cell biocatalysis

10 mL reaction mixtures contained 25 mM substrate (S17–S26) dissolved in Tris-HCl buffer with methanol (5% v/v), 1.5 equivalent of glucose, 10 mg GDH, 0.2 mM $NADP^+$, and the reactions were performed at 30 °C and 180 rpm. Reactions were started by addition of 10 $g \cdot L^{-1}$ dry cells of $HAPMO_{pf}$. Samples were withdrawn from the reaction mixture at different time intervals, and then extracted with equal volume of ethyl acetate supplemented with 1 mM dodecane as an external standard. The organic phase was isolated and dried over anhydrous Na_2SO_4, and the conversion ratio and enantioselectivity were determined by HPLC/GC as described in the supplementary information.

Results and discussion

Genome mining of HAPMOs

P. fluorescens ACB utilizes 4-hydroxyacetophenone as the sole carbon and energy source [1], from which $HAPMO_{pf\ ACB}$, a classic HAPMO was cloned and characterized [9]. $HAPMO_{pf\ ACB}$ produces optically pure enantiomers using sulfides as substrates [23,24], and therefore is regarded as an appropriate probe for genome date mining. Herein, UniProt/Swiss-Prot database was searched using $HAPMO_{pf\ ACB}$ (AAK54073.1) as a search query. Interestingly, two BVMOs were identified from *P. fluorescens* with 72% and 57% amino acid sequence identities. Both BVMO encoding genes were successfully expressed in a partially soluble form and displayed measurable activity (>1% conversion) toward 4-hydroxyacetophenone and phenyl methyl sulfoxide (Table 1), and were designated as $HAPMO_{pf}$ (A0A159ZVV3) and $HAPMO_{pf1}$ (A0A379IFA4), respectively. $HAPMO_{pf}$ (A0A159ZVV3), displaying better soluble expression and conversion ratio than $HAPMO_{pf1}$ (A0A379IFA4), was chosen for further investigation.

Sequence analysis of $HAPMO_{pf}$

A phylogenetic analysis of $HAPMO_{Pf}$ and known BVMOs with different catalytic functions was performed. As shown in Fig. 1, $HAPMO_{Pf}$ is positioned in the same branch as the classical 4-hydroxyacetophenone monooxygenase from *P. fluorescens* ACB ($HAPMO_{pf\ ACB}$) [23], sharing an overall sequence identity of 72% (Fig. 1). Other known enzymes in the branch include HAPMO from P. *putida* JD1($HAPMO_{pp}$) [10]. Among reported BVMOs, $HAPMO_{Pf}$ displays merely 20% identity with CHMO from *Acinetobacter* sp. NCIMB 9871 [28], an enzyme exhibiting broad substrate spectrum in the biooxidation of (cyclic) ketones. The sequence identity between $HAPMO_{Pf}$ and PAMO from *Thermobifida fusca* [11] with aromatic ketones oxidation activity is only 22%. Multiple sequence alignment between $HAPMO_{Pf}$ and seven well-studied type I BVMOs revealed that $HAPMO_{Pf}$ contains a short BVMO fingerprint (FxGxxxHTxxW[P/D]) and two Rossmann fold domains (GxGxx[G/A]) [29] responsible for cofactor binding [8] (Fig. 2). Above results indicate that $HAPMO_{Pf}$ is a new HAPMO ortholog.

Characterization of $HAPMO_{Pf}$

Based on SDS-PAGE analysis, recombinant $HAPMO_{Pf}$ existed in both supernatant and precipitate, yielding a prominent band at 70 kDa (Fig. 3A). The specific activity of crude enzyme toward S17 was 0.87 $U{\cdot}mg^{-1}$. Through nickel affinity chromatography, purified $HAPMO_{Pf}$ was obtained with recovery ratio of 90.5% and specific activity of 1.91 $U{\cdot}mg^{-1}$ toward S17. Purified $HAPMO_{Pf}$ displayed activity with NADPH as cofactor and no activity with NADH, indicating $HAPMO_{Pf}$ is an NADPH-dependent BVMO.

In previous reports, the optimum pH of most BVMOs falls in alkaline range [11,13,30]. As illustrated in Fig. 3B, the optimum pH of $HAPMO_{Pf}$ was observed in pH 9.0 Tris-HCl buffer. The alkaline pH preference of $HAPMO_{Pf}$ is similar to other HAPMOs, such as $HAPMO_{pp}$ (pH 8.0) [10] and $HAPMO_{pf\ ACB}$ (pH 9.0) [23]. It should be noted that the activity of $HAPMO_{Pf}$ reduced dramatically under acidic conditions, and less than 30% relative activity was remained at pH 6.5. Influence of temperature on the activity of $HAPMO_{Pf}$ was also explored. The activity of $HAPMO_{Pf}$ gradually increased from 20 to 30 °C and reached the highest activity at 30 °C (Fig. 3C). At 35 °C, 95% relative activity was measured, whereas only 50% of relative activity was remained at 40 °C. The thermostability of $HAPMO_{Pf}$ was also monitored by measuring the residual activity after incubation at different temperatures. After approximately 24 h at 30 °C (pH 9.0), the residual activity was about 55%, indicating that the thermostability of $HAPMO_{Pf}$ is moderate at 30 °C (pH 9.0) (Fig. 3D). $HAPMO_{Pf}$ was unstable at 40 °C, and less than 5% of residual activity was detected after incubation at 40 °C for 30 min. The half-life of $HAPMO_{Pf}$ was calculated to be 24 h at 30 °C according to the Arrhenius deactivation equation. In contrast, the half-life of $HAPMO_{pp}$ at 30 °C is less than 5 h [10], indicating $HAPMO_{Pf}$ has better thermostability than $HAPMO_{pp}$. Moreover, appropriate amount of purified $HAPMO_{Pf}$ was incubated with different organic solvents (5%, v/v) for 2 h, and the effect of different organic solvents were also investigated (Fig. S1), Methanol had little effect on the activity of $HAPMO_{Pf}$, and over 85% relative activity was retained, whereas ethanol, DMSO and acetonitrile significantly affected its activity, resulting in about 50% relative activity. Acetone and *i*-PrOH had the most destructive effects on $HAPMO_{Pf}$, leading to the loss of about 70% activity.

Substrate specificity of $HAPMO_{Pf}$

In order to explore the substrate specificity of $HAPMO_{Pf}$, a variety of ketone and thioether substrates, including (i) aromatic ketones, (ii) thioethers, and (iii) aliphatic ketones, were investigated (Fig. 4 and Table 2). Substrate spectra of $HAPMO_{pf\ ACB}$ [23,24] and $HAPMO_{pp}$ [10] have been reported, showing that these enzymes preferentially oxidize acetophenone derivatives.

Oxidation of aromatic ketones

So far, only a few BVMOs, such as $HAPMO_{pf\ ACB}$, have been tested for conversion of aromatic compounds [9]. Here, acetophenone (S10), phenylacetone (S11), 4-phenyl-2-butanone (S12) and acetophenone derivatives including three hydroxyacetophenone substrates (*para, meta* and *ortho*) (S1-S3) and six *para*-substituted-acetophenones substrates (F-, Cl-, NH_2-, CH_3-, CH_3O-, NO_2-) (S4-S9) were investigated. As illustrated in Fig. 4, a decrease in activity of $HAPMO_{Pf}$ was observed along with the elongation of side chain of aromatic ring, such as S10–S12. The *para, meta* and *ortho*-hydroxyacetophenones (S1-S3) could also be oxidized by $HAPMO_{Pf}$, which displayed the highest specific activity toward S1 (1.47 $U{\cdot}mg^{-1}$). Similar to $HAPMO_{pf\ ACB}$, $HAPMO_{Pf}$ preferred *para*-hydroxyacetophenones (S1) to *meta*- and *ortho*-hydroxyacetophenone substrates (S1–S3) [9], confirming it belongs to the typical 4-hydroxyacetophenone monooxygenase subfamily. $HAPMO_{Pf}$ exhibited moderate activities of 1.04 $U{\cdot}mg^{-1}$ and 0.90 $U{\cdot}mg^{-1}$ toward 4-aminoacetophenone (S6) and 4-methylacetophenone (S7), respectively. The activity for other *para*-substituted acetophenones (S4, S5, S8) were 0.35–0.39 $U{\cdot}mg^{-1}$. Among six *para*-substituted-acetophenones substrates (F-, Cl-, NH_2-, CH_3-, CH_3O-, NO_2-) (S4-S9), like $HAPMO_{pf\ ACB}$, $HAPMO_{Pf}$ showed no activity toward 4-nitroacetophenone (S9). These

Table 1
Gene mining of HAPMOs for enantioselective sulfoxidation[a].

Name	AccessionNumber	Microorganism	Sequenceidentity (%)	Conv. (%)[a] &%*ee* (config.)[b]
$HAPMO_{pf\ ACB}$	AAK54073.1	*Pseudomonas fluorescens* ACB	100	NA[c] (99 *S*)
$HAPMO_{pf}$	A0A159ZVV3	*Pseudomonas fluorescens*	72	99(99 *S*)
$HAPMO_{pf1}$	A0A379IFA4	*Pseudomonas fluorescens*	57	<1

[a] The 500 μL reaction mixture contained diluted crude enzyme extracts, 1 mM NADPH, 1 mM methyl phenyl sulfide, 2% (vol/vol) methanol, and Tris-HCl (100 mM, pH 9.0) at 30 °C.
[b] Conversion and enantiomeric excess were determined by chiral HPLC.
[c] NA: not available.

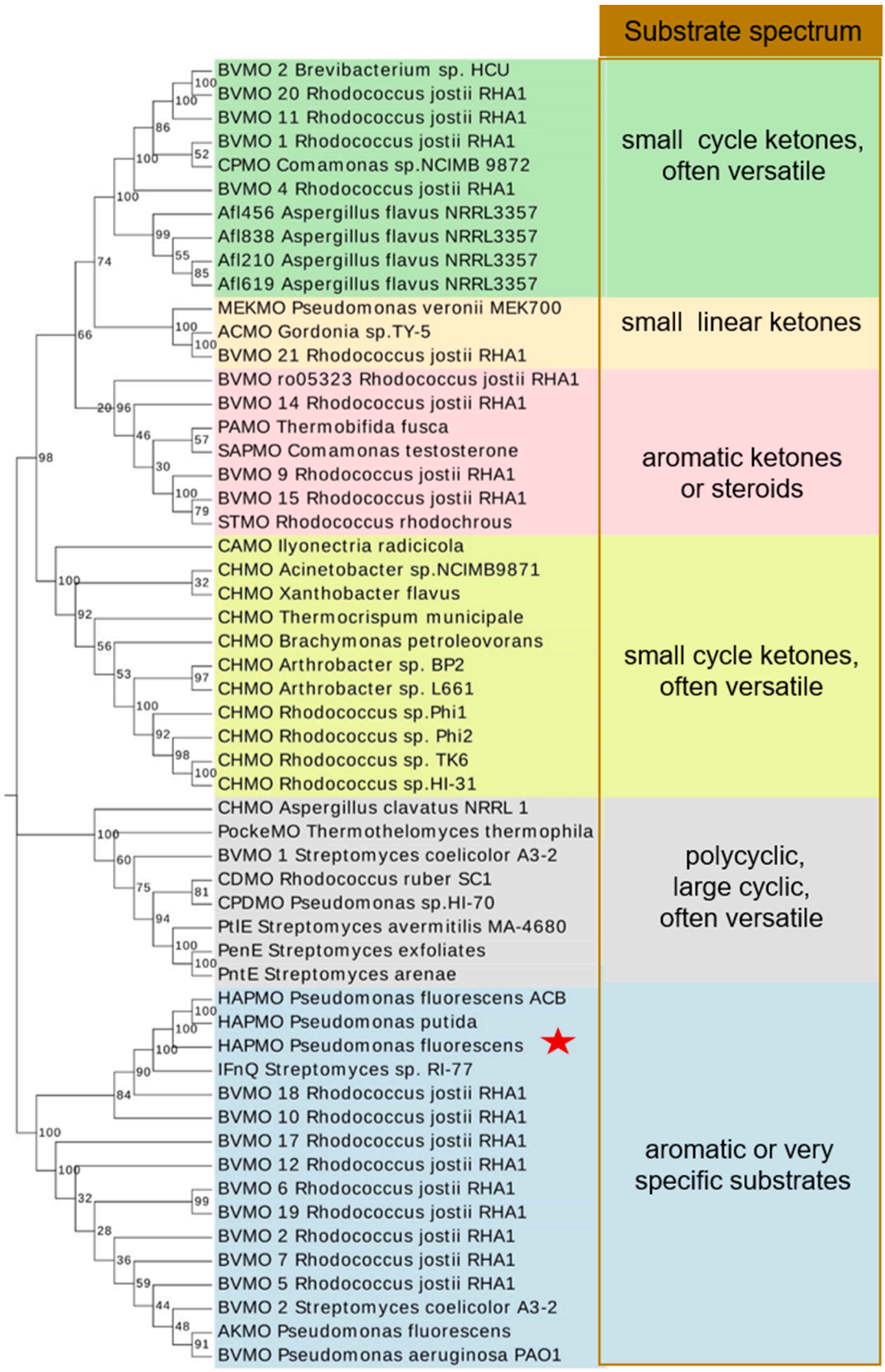

Fig. 1. Phylogenetic analysis of $HAPMO_{Pf}$ and other known BVMOs. Amino acid sequences were retrieved from NCBI database (The bootstrap values were based on 1000 replicates).

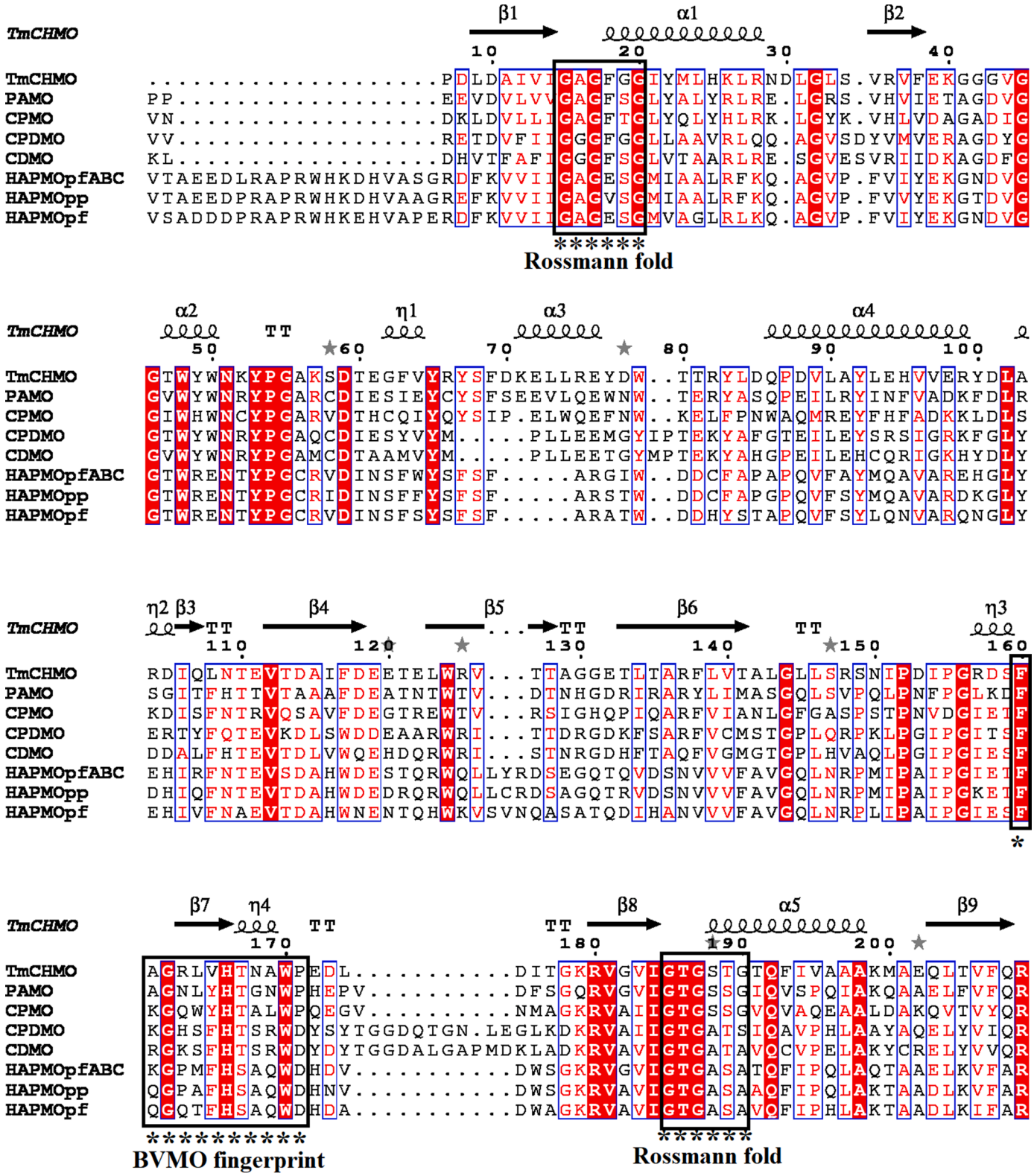

Fig. 2. Multiple sequence alignment of HAPMO$_{pf}$ and seven typical BVMOs from different clades. Two Rossmann-fold motifs (GxGxxG/A) and BVMO fingerprint of Type I BVMOs (FxGxxxHxxxWP/D) were annotated.

results indicate that substitutions on the phenyl ring is crucial for substrate recognition.

Sulfoxidation of sulfide compounds

In addition to oxidation of ketones, some BVMOs such as HAPMO$_{pf}$ $_{ACB}$ [23], and enantiocomplementary *Ra*BVMO and *Am*BVMO [32], can catalyze the sulfoxidation of various sulfide compounds including aromatic sulfides, which are important chiral building blocks in pharmaceutical chemistry [5,15,31,32]. Here, various thioethers S17–S29 were interrogated as possible substrates by determining activity and

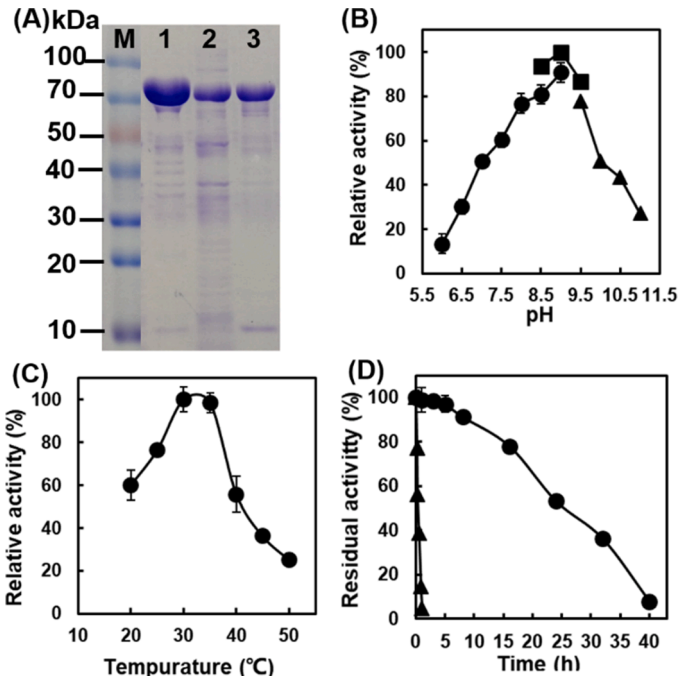

Fig. 3. (A) SDS-PAGE analysis of recombinant expression of HAPMO$_{Pf}$ in *E. coli* BL21 (DE3). M: protein marker; 1: HAPMO$_{Pf}$ cell extract supernatant; 2: HAPMO$_{Pf}$ cell extract sediment; 3: purified enzyme. **(B)** Effect of pH on HAPMO$_{Pf}$: (●): sodium phosphate buffer (pH 6.0–9.0), (■): Tris–HCl buffer (pH 8.0–9.5), (▲): Glycine-NaOH buffer (pH 9.0–11.0); **(C)** Effect of temperature on HAPMO$_{Pf}$; **(D)** Thermostability of HAPMO$_{Pf}$: (●): 30 °C, (▲): 40 °C.

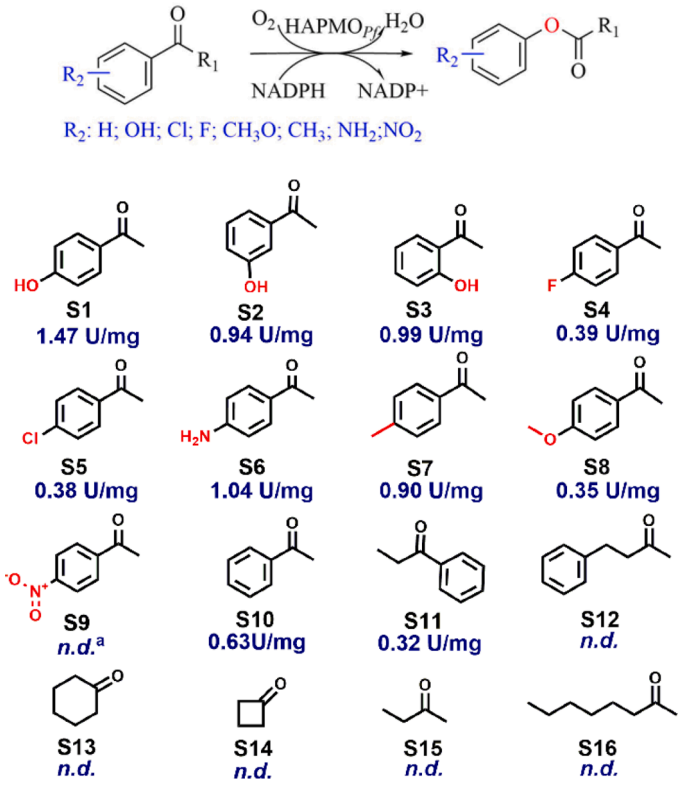

Fig. 4. Specific activity of HAPMO$_{Pf}$ toward ketone substrates. Specific activity was determined with 5 mM substrate using purified enzymes at pH 9.0 and 30 °C. [a]: *n.d*, no activity was detected.

enantiomeric excess (*ee*) of the products. As illustrated in Table 2, HAPMO$_{Pf}$ catalyzed the oxidation of prochiral S17 with an activity of 1.91 U·mg^{-1} and excellent enantioselectivity of > 99% (*S*) *ee*. For all the tested methyl phenyl sulfide derivatives, HAPMO$_{Pf}$ exhibited increased activities following the order of *ortho-* < *meta-* and *para*-positions, except for substrates with amino substituent (S27–S29). In all cases, (*S*)-sulfoxides were produced from thioether derivatives (S18-S29). Except for *para*-chloromethyl phenyl sulfide (S20) with 97% *ee* (*S*) and *para*-methoxymethyl phenyl sulfide (S26) with 95% *ee* (*S*), perfect enantiomeric excesses (*ee* ≥ 99%) were achieved for other sulfides tested, indicating strict stereo-preference for S17 and derivatives. HAPMO$_{Pf\ ACB}$ has been reported to oxidize S18 with low enantioselectivity of 44% (*S*), while S19 and S20 in 96% (*S*) and 93% (*S*), respectively [23]. In addition, HAPMO$_{Pf\ ACB}$ showed higher selectivity for phenyl methyl sulfides carrying *para*-electron donating than electron-withdrawing ones [9]. Whereas HAPMO$_{Pf}$ displayed high selectivity and moderate activity for all tested substrates. These results suggested that the activity of HAPMO$_{Pf}$ is barely affected by the substituents and their positions on phenyl ring, and is a promising biocatalyst with broad application prospects.

Oxidation of aliphatic ketones

Linear and cyclic alkyl ketones are potential substrates for BVMOs [8,33]. HAPMO$_{Pf}$ showed no activity toward cyclic ketones (S13 and S14) and aliphatic ketones (S15 and S16) (Fig. 4), suggesting HAPMO$_{Pf}$ has strict substrate preference for aromatic compounds.

Kinetic parameter analysis

The effect of hydroxy group on K_M and k_{cat} values of HAPMO$_{Pf}$ toward hydroxyacetophenone compounds was explored, including 2-hydroxyacetophenone (S3), 3-hydroxyacetophenone (S2), 4-hydroxyacetophenone (S1) (Table 3 and Fig. S2). These three acetophenone derivatives could be oxidized by HAPMO$_{Pf}$. Among them, the highest K_M values of 1.43 mM was determined for S2 with *meta*-substituted hydroxy, followed by K_M of 0.457 mM toward *ortho*-substrate (S3). The lowest K_M value of 0.025 mM was obtained with S1, indicating HAPMO$_{Pf}$ has the highest binding affinity toward 4-hydroxyacetophenone. This result is consistent with HAPMO$_{Pf\ ACB}$ and HAPMO$_{pp}$ [10,24]. The k_{cat} values of three hydroxyacetophenone compounds follow the order of *para* > *meta* > *ortho*, which is different from HAPMO$_{Pf\ ACB}$ and HAPMO$_{pp}$ [10,24], indicating the substituting position on aromatic ring (*para, meta*, or *ortho*) is important for substrate conversion (Table 3). The substrate binding affinity of HAPMO$_{Pf\ ACB}$ toward *para*-substituted acetophenones depends on the electronic properties of substituents, demonstrating better binding of ketones with electron-donating groups than those with electron-withdrawing groups [23]. HAPMO$_{Pf}$ catalyzed the oxidation of different *para*-substituted acetophenones were as summarized in Table 3. Compared with HAPMO$_{Pf\ ACB}$ and HAPMO$_{pp}$ [10,24], HAPMO$_{Pf}$ has higher K_M values and lower k_{cat} values for *para*-substituted acetophenones (Table 3). Interestingly, for 4-chloroacetophenone (S5), HAPMO$_{Pf}$ exhibited a high K_M value of 4.74 mM, HAPMO$_{Pf\ ACB}$ showed no activity, while HAPMO$_{pp}$ has a low K_M of 0.14 mM. 4-Nitroacetophenone (S9) could not be converted by HAPMO$_{Pf}$, which is similar to HAPMO$_{Pf\ ACB}$, whereas HAPMO$_{pp}$ could oxidizes S9 with a K_M value of 0.31 mM, indicating that three enzymes have distinct catalytic characteristics. The lowest K_M value was observed with 4-aminoacetophenone (S6), with a K_M value of 0.016 mM. For 4-fluoro-(S4) and 4-chloroacetophenone (S5), the highest K_M values of 4.08 and 4.74 mM were determined followed by substrates with hydrophobic substituents (4-methyl-(S7) and 4-methoxy-(S8)), indicating that methyl, methoxy, fluoro and chloro groups possess a positive inductive or mesomeric effect [34]. In summary, HAPMO$_{Pf}$ showed lower K_M values for acetophenones with electron-donating substituents (NH_2, CH_3, CH_3O) (S6–S8) compared with those with electron-withdrawing substituents (F, Cl) (S4, S5). The k_{cat} values of different *para*-substitution were also analyzed. Except for 4-methylacetophenone (S7)

Table 2
HAPMO$_{Pf}$ catalyzed oxidation of methyl phenyl sulfide derivatives X–Ph–S–CH_3 (S17–S29) to corresponding sulfoxides.

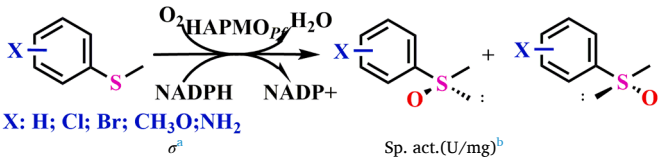

X: H; Cl; Br; CH_3O;NH_2

Substrate entry	X	σ[a]	Sp. act.(U/mg)[b]	% *ee*	Config.[c]
S17	H	0	1.91	99	*S*
S18	*o*-Cl	–	0.37	99	*S*
S19	*m*-Cl	0.37	0.85	99	*S*
S20	*p*-Cl	0.23	0.81	97	*S*
S21	*o*-Br	–	0.87	99	*S*
S22	*m*-Br	0.39	0.83	99	*S*
S23	*p*-Br	0.23	0.74	99	*S*
S24	*o*-CH_3O	–	0.43	99	*S*
S25	*m*-CH_3O	0.12	0.91	99	*S*
S26	*p*-CH_3O	−0.27	0.89	95	*S*
S27	*o*-NH_2	–	0.13	99	*S*
S28	*m*-NH_2	−0.16	0.11	99	*S*
S29	*p*-NH_2	−0.66	0.10	99	*S*

[a] σ values taken from Ref. [34].
[b] Specific activity was determined at pH 9.0 and 30 °C with 2 mM substrate using the purified enzyme. One unit U corresponds to 1 μmol product formed per min.
[c] Enantiomeric excess determined by HPLC.

Table 3
Kinetic parameters of HAPMO$_{Pf}$ toward acetophenone derivatives (S1-S9) and methyl phenyl sulfide (S17).

Entry	Substrate	HAPMO$_{Pf}$			HAPMO$_{pp}$ [10]			HAPMO$_{Pf\ ACB}$ [24]		
		K_M(mM)	k_{cat}(s^{-1})	k_{cat}/K_M(s^{-1}.mM^{-1})	K_M(mM)	k_{cat}(s^{-1})	k_{cat}/K_M(s^{-1}.mM^{-1})	K_M(mM)	k_{cat}(s^{-1})	k_{cat}/K_M(s^{-1}.mM^{-1})
S1	**4-Hydroxyacetophenone**	0.025	0.6	24.00	0.038	9.8	257.89	9.2×10^{-3}	12.6	1.36×10^{3}
S2	**3-Hydroxyacetophenone**	1.430	3.0	2.09	0.246	8.1	32.92	1.400	4.8	3.42
S3	**2′-Hydroxyacetophenone**	0.457	3.1	6.78	0.121	21.2	175.20	0.610	6.7	10.98
S4	**4-Fluoroacetophenone**	4.082	1.6	0.39	0.208	1.3	6.25	1.000	0.6	0.60
S5	**4-Chloroacetophenone**	4.746	1.4	0.29	0.140	1.6	11.42	NA[a]	NA	NA
S6	**4-Aminoacetophenone**	0.016	0.5	31.25	5.6×10^{-3}	8.2	1.46×10^{3}	0.82×10^{-3}	12.7	15.48×10^{3}
S7	**4-Methylacetophenone**	1.487	3.2	2.15	0.241	4.4	18.25	0.160	6.3	39.37
S8	**4-Methoxyacetophenone**	0.768	0.2	0.26	0.199	1.2	6.03	0.540	1.7	3.14
S9	**4-Nitroacetophenone**	NA	NA	NA	0.313	2.6	8.30	NA	NA	NA
S17	**Methyl phenyl sulfide**	2.733	3.7	1.35	Na	Na	Na	1.400	4.7	3.35

[a] NA: no activity.

(k_{cat} = 3.2 s^{-1}), the k_{cat} values for *para*-substituted-acetophenones (S4–S6, and S8) fall in the range of 0.19–1.6 s^{-1}, indicating that substitutions on the phenyl ring have a moderate effect. Interestingly, 4-nitroacetophenone (S9) could not be oxidized by HAPMO$_{Pf}$ and HAPMO$_{pf\ ACB}$, whereas HAPMO$_{pp}$ has a k_{cat} value of 2.6 s^{-1} toward S9. Therefore, all three HAPMOs show the highest activities toward acetophenones bearing *para*-electron donating substituents. These data led us to understand the catalytic properties of HAPMO$_{pf}$ toward acetophenone substrates. Among them, lower K_M values and similar k_{cat} values were observed with 4-hydroxyacetophenone (S1) (0.025 mM and 0.6 s^{-1}) and 4-aminoacetophenone (S6) (0.016 mM and 0.5 s^{-1}), which are the preferable substrates of HAPMO$_{Pf}$.

For S17 (Table 3), HAPMO$_{Pf}$ showed a k_{cat} of 3.7 s^{-1} and K_M of 2.73 mM, HAPMO$_{pf\ ACB}$ exhibited a K_M value of 1.40 mM and k_{cat} values of 4.7 s^{-1} [24], whereas HAPMO$_{pp}$ could not catalyze S17 [10]. For S17, HAPMO$_{pf\ ACB}$ has an approximately 2-fold lower K_M value compared with HAPMO$_{Pf}$, while similar k_{cat} values, leading to lower k_{cat}/K_M of HAPMO$_{Pf}$. The above results show that HAPMO$_{Pf}$ is a potential biocatalyst for the synthesis of chiral sulfoxides and esters, due to its broad substrate spectrum and high enantioselectivity toward *ortho*-, *meta*- and *para*-substituted methyl phenyl sulfides.

Homologous modeling and molecular docking analysis of HAPMO$_{Pf}$

The structure model of HAPMO$_{Pf}$ was constructed by Robetta [35] with a confidence coefficient of 0.85. The predicted structure was evaluated by SAVES v6.0 [36], and the ramachandran plot analysis shows that 90% residues are located in the reasonable region (Fig. S3). Molecular docking analysis was performed by Discovery studio 4.5. To understand the binding orientation of S17 in the active site of HAPMO$_{Pf}$. Substrate S17 was docked into the binding pocket of HAPMO$_{Pf}$, and a range of binding poses were obtained. According to the scoring and binding mode, the best docking conformation was selected and depicted in Fig. 5. The volume of substrate binding pocket of HAPMO$_{Pf}$ was calculated to be about 75.8 $Å^3$. The small binding pocket of HAPMO$_{Pf}$ is favorable for its excellent enantioselectivity. Key residues interactions between enzyme and S17 were also analyzed as illustrated in Fig. 5. S17 was well-accommodated into the active center by a amide−π stacked interaction of V544, strong hydrophobic interactions with surrounding residues (R440 and I549), and multiple van der waal interactions with several residues (Q275 and V545) in HAPMO$_{Pf}$ (Fig. 5). The distance between the sulfur atom of S17 and the distal oxygen of the flavin peroxy-anion intermediate was determined to be 3.2 Å in HAPMO$_{Pf}$, which allows S17 to get close to the hydroperoxo group. In the binding pose shown in Fig. 5, the sulfur atom of S17 is close to the FAD cofactor, while the phenyl ring is away from the hydroperoxo group, thus leaving

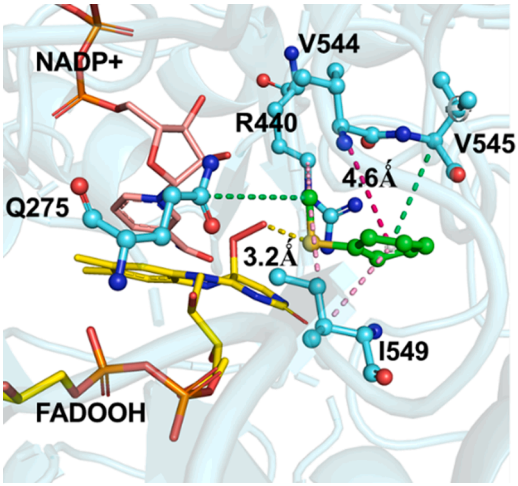

Fig. 5. Poses of methyl phenyl sulfide docked in modeled structure of HAPMO$_{Pf}$. The substrate methyl phenyl sulfide is shown in green color, the FAD prosthetic group in yellow, $NADP^+$coenzyme in red, and amino acid residues in blue. Hot pink dashed line: amide−π stacked interaction between amino acid V544 and benzene ring of methyl phenyl sulfide in 4.6 Å; pink dashed lines: alkyl interactions between amino acids R440/I549 and methyl of methyl phenyl sulfide in 4.73 Å and 5.0 Å, respectivly; green dashed lines: van der waal interactions between amino acids Q275/V545 and methyl phenyl sulfide in 4.8 Å and 5.1 Å, respectivly; yellow dashed line: distance between distal oxygen of the flavin peroxy-anion intermediate and sulfur atom of methyl phenyl sulfide in 3.2 Å.

the *pro*-(*S*) lone pair available for reaction with the FAD moiety to result in excellent (*S*)-enantioselectivity. Molecular docking and interactions analysis provide substantial evidence for the excellent enantioselectivity of HAPMO$_{Pf}$.

Sulfoxidation catalyzed by HAPMO$_{Pf}$ in whole-cell biocatalysis

The oxidation of aromatic sulfides by HAPMO$_{Pf}$ (Table 4), was coupled with glucose dehydrogenase (GDH) for NADPH regeneration utilizing glucose. All reactions were carried out in a Tris-HCl buffer at pH 9.0. As shown in Table 4, for S17, moderate conversion (79.3%) was obtained after 24 h, resulting in (*S*)-methyl phenyl sulfoxide with 99% *ee*. For methyl phenyl sulfides with electron-withdrawing groups (Cl and Br, S18–S23), (*S*)-sulfoxides were mainly produced with strict enantioselectivity of 99%, except for *para*-chloromethyl phenyl sulfide (S20) with 97% *ee* (*S*). Conversion ratios toward substrates with *meta*-, *ortho*- and *para*-chloro substituents (S18–S20), followed the order of *para*-chloro (S20) > *ortho*-chloro (S19) > *meta*-chloro (S18). Specifically, low conversion (34.4%) was obtained with S18, while high conversion ratios of 83.5% and 88.9% were achieved with S19 and S20, respectively. The conversion ratios of substrates with bromo- at *meta*- and *ortho*- positions (S21, S22) were higher (85.8%, 89.8%) than that of *para*-bromo substrate (S23) (72.6%). For methyl phenyl sulfides with electron-donating groups (OCH_3, S24–S26), both *meta*- and *para*-methoxy substrates (S25, S26) were oxidized with high conversion ratios (93.4%, 89.9%), with a low conversion ratio (41.8%) was observed for *ortho*-methoxy methyl phenyl sulfide (S24). No further oxidation of sulfoxides to sulfones was determined in all the reactions.

Conclusions

In summary, a novel HAPMO$_{Pf}$ from *Pseudomonas fluorescens* FW300-N2E2 was identified by genome mining. After HAPMOs from *P. fluorescens* ACB and *P. putida* JD1 and PAMO from *T. fusca*, this HAPMO$_{Pf}$ represents the fourth described BVMO capable of preferentially oxidizing aromatic ketones. Interestingly, HAPMO$_{Pf}$ has a broad substrate spectrum toward *para*-substituted aromatic ketones. Furthermore, HAPMO$_{Pf}$ catalyzes the oxidation of various methyl phenyl sulfide substrates to produce (*S*)-enantiomers, demonstrating its potential application in a wide variety of enantioselective biooxidation reactions.

Table 4
Biotransformation of sulfides S17-S26 to the corresponding (*S*)-sulfoxides catalyzed by HAPMO$_{Pf}$ -based whole-cell biocatalysts.

Sulfides[a]	Conv. (%)[b]	*ee* (%)[b]
S17	79.3	99
S18	34.4	99
S19	83.5	99
S20	88.9	97
S21	85.8	99
S22	89.8	99
S23	72.6	99
S24	41.8	99
S25	93.4	99
S26	89.9	95

[a] A 10 mL reaction system containing enzyme and sulfides (25 mM) in Tris-HCl buffer (100 mM, pH 9.0) was performed at 30 °C for 24 h.
[b] Conversion and enantiomeric excess were determined by HPLC.

Availability of data and materials

All data generated or analysed during this study are included in this published article and its supplementary information files.

Ethical statement

This article does not contain any studies with human participants or animals performed by any of the authors.

CRediT authorship contribution statement

Shiyu Wei: Investigation, Data curation, Writing – original draft, Validation. **Guochao Xu:** Methodology, Conceptualization, Writing – review & editing. **Jieyu Zhou:** Formal analysis. **Ye Ni:** Conceptualization, Supervision, Funding acquisition, Writing – review & editing.

Declaration of Competing Interest

The authors declare that they have no known competing financial interests or personal relationships that could have appeared to influence the work reported in this paper.

Data availability

Data will be made available on request.

Funding

This work was supported by National Key R&D Program (2021YFC2102700, 2018YFA0901700, 2019YFA0906401), National Natural Science Foundation of China (22077054, 22078127), and National First-Class Discipline Program of Light Industry Technology and Engineering (LITE2018-07).

Supplementary materials

Supplementary material associated with this article can be found, in the online version, at doi:10.1016/j.mcat.2022.112496.

References

[1] F.K. Higson, D.D. Focht, Bacterial degradation of ring-chlorinated acetophenones, Appl. Environ. Microbiol. 56 (1990) 3678–3685.

[2] R.E. Cripps, The microbial metabolism of acetophenone. Metabolism of acetophenone and some chloroacetophenones by an *Arthrobacter* species, Biochem. J. 152 (1975) 233–241.

[3] J. Havel, W. Reineke, Microbial degradation of chlorinated acetophenones, Appl. Environ. Microbiol. 59 (1993) 2706–2712.

[4] K.H. Jones, P.W. Trudgill, D.J. Hopper, 4-Ethylphenol metabolism by *Aspergillus fumigatus*, Appl. Environ. Microbiol. 60 (1994) 1978–1983.

[5] M. Bucko, P. Gemeiner, A. Schenkmayerova, T. Krajcovic, F. Rudroff, M. D. Mihovilovic, Baeyer-Villiger oxidations: biotechnological approach, Appl. Microbiol. Biotechnol. 100 (2016) 6585–6599.

[6] C.E. Paul, D. Eggerichs, A.H. Westphal, D. Tischler, W.J.H. van Berkel, Flavoprotein monooxygenases: versatile biocatalysts, Biotechnol. Adv. 51 (2021), 107712.

[7] W.J.H. van Berkel, N.M. Kamerbeek, M.W. Fraaije, Flavoprotein monooxygenases, a diverse class of oxidative biocatalysts, J. Biotechnol. 124 (2006) 670–689.

[8] M.J.L.J. Fürst, A. Gran-Scheuch, F.S. Aalbers, M.W. Fraaije, Baeyer–villiger monooxygenases: tunable oxidative biocatalysts, ACS Catal. 9 (2019) 11207–11241.

[9] N.M. Kamerbeek, M.J. Moonen, J.G. Van Der Ven, W.J. Van Berkel, M.W. Fraaije, D.B. Janssen, 4-Hydroxyacetophenone monooxygenase from *Pseudomonas fluorescens* ACB. A novel flavoprotein catalyzing Baeyer-Villiger oxidation of aromatic compounds, Eur. J. Biochem. 268 (2001) 2547–2557.

[10] J. Rehdorf, C.L. Zimmer, U.T. Bornscheuer, Cloning, expression, characterization, and biocatalytic investigation of the 4-hydroxyacetophenone monooxygenase from *Pseudomonas putida* JD1, Appl. Environ. Microbiol. 75 (2009) 3106–3114.

[11] M.W. Fraaije, J. Wu, D.P. Heuts, E.W. van Hellemond, J.H. Spelberg, D.B. Janssen, Discovery of a thermostable Baeyer-Villiger monooxygenase by genome mining, Appl. Microbiol. Biotechnol. 66 (2005) 393–400.

[12] Y. Zhang, Y.Q. Wu, N. Xu, Q. Zhao, H.L. Yu, J.H. Xu, Engineering of cyclohexanone monooxygenase for the enantioselective synthesis of (*S*)-omeprazole, ACS Sustain. Chem. Eng. 7 (2019) 7218–7226.

[13] Y. Zhang, F. Liu, N. Xu, Y.Q. Wu, Y.C. Zheng, Q. Zhao, G. Lin, H.L. Yu, J.H. Xu, Discovery of two native Baeyer-Villiger monooxygenases for asymmetric synthesis of bulky chiral sulfoxides, Appl. Environ. Microbiol. 84 (2018) e00638-18.

[14] S. Anselmi, N. Aggarwal, T.S. Moody, D. Castagnolo, Unconventional biocatalytic approaches to the synthesis of chiral sulfoxides, ChemBioChem 22 (2021) 298–307.

[15] T. Jia, M. Wang, J. Liao, Chiral sulfoxide ligands in asymmetric catalysis, Top. Curr. Chem. 377 (2019) 8.

[16] T. Matsui, Y. Dekishima, M. Ueda, Biotechnological production of chiral organic sulfoxides: current state and perspectives, Appl. Microbiol. Biotechnol. 98 (2014) 7699–7706.

[17] H.R. Luckarift, H. Dalton, N.D. Sharma, D.R. Boyd, R.A. Holt, Isolation and characterisation of bacterial strains containing enantioselective DMSO reductase activity: application to the kinetic resolution of racemic sulfoxides, Appl. Microbiol. Biotechnol. 65 (2004) 678–685.

[18] H. Zheng, Y. Zhou, X. Lin, Q. Wu, Recent developments in protein engineering and catalytic oxidations of Baeyer-Villiger monooxygenase, Chin. J. Org. Chem. 39 (2019) 903–915.

[19] R.A. Sheldon, J.M. Woodley, Role of biocatalysis in sustainable chemistry, Chem. Rev. 118 (2018) 801–838.

[20] A.T. Li, J.D. Zhang, H.L. Yu, J. Pan, J.H. Xu, Significantly improved asymmetric oxidation of sulfide with resting cells of *Rhodococcus* sp. in a biphasic system, Process Biochem. 46 (2011) 689–694.

[21] C. Willrodt, J.A.D. Gröning, P. Nerke, R. Koch, A. Scholtissek, T. Heine, A. Schmid, B. Bühler, D. Tischler, Highly efficient access to (*S*)-sulfoxides utilizing a promiscuous flavoprotein monooxygenase in a whole-cell biocatalyst format, ChemCatChem 12 (2020) 4664–4671.

[22] J. Yang, Y. Wen, L. Peng, Y. Chen, X. Cheng, Y. Chen, Identification of MsrA homologues for the preparation of (*R*)-sulfoxides at high substrate concentrations, Org. Biomol. Chem. 17 (2019) 3381–3388.

[23] G. de Gonzalo, D.E. Torres Pazmiño, G. Ottolina, M.W. Fraaije, G. Carrea, 4-Hydroxyacetophenone monooxygenase from *Pseudomonas fluorescens* ACB as an oxidative biocatalyst in the synthesis of optically active sulfoxides, Tetrahedron Asymmetry 17 (2006) 130–135.

[24] N.M. Kamerbeek, A.J. Olsthoorn, M.W. Fraaije, D.B. Janssen, Substrate specificity and enantioselectivity of 4-hydroxyacetophenone monooxygenase, Appl. Environ. Microbiol. 69 (2003) 419–426.

[25] K. Katoh, J. Rozewicki, K.D. Yamada, MAFFT online service: multiple sequence alignment, interactive sequence choice and visualization, Brief. Bioinform. 20 (2017) 1160–1166.

[26] S. Kumar, G. Stecher, M. Li, C. Knyaz, K. Tamura, Mega X: molecular evolutionary genetics analysis across computing platforms, Mol. Biol. Evol. 35 (2018) 1547–1549.

[27] J. Sambrook, E.F. Fritsch, T. Maniatis. Molecular Cloning: A Laboratory Manual 2nd ed., 28, Cold Spring Harbor Laboratory Press, 1990, pp. 201–212, eua1989, Studies in Christian Ethics.

[28] M. Wright, C. Knowles, F. Petit, R. Furstoss, Enantioselective inhibition studies of the cyclohexanone monooxygenase from *Acinetobacter* sp. NCIMB 9871, Biotechnol. Lett. 16 (1994) 1287–1292.

[29] M.W. Fraaije, N.M. Kamerbeek, W.J.H. van Berkel, D.B. Janssen, Identification of a Baeyer–Villiger monooxygenase sequence motif, FEBS Lett. 518 (2002) 43–47.

[30] A. Gran-Scheuch, M. Trajkovic, L. Parra, M.W. Fraaije, Mining the genome of streptomyces leeuwenhoekii: two new Type I Baeyer-Villiger monooxygenases from *Atacama desert*, Front. Microbiol. 9 (2018) 1609.

[31] J. Han, V.A. Soloshonok, K.D. Klika, J. Drabowicz, A. Wzorek, Chiral sulfoxides: advances in asymmetric synthesis and problems with the accurate determination of the stereochemical outcome, Chem. Soc. Rev. 47 (2018) 1307–1350.

[32] S.Y. Wei, Y.F. Liu, J.Y. Zhou, G.C. Xu, Y. Ni, Two enantiocomplementary Baeyer-Villiger monooxygenases newly identified for asymmetric oxyfunctionalization of thioether, Mol. Catal. 513 (2021), 111784.

[33] G. de Gonzalo, G. Ottolina, F. Zambianchi, M.W. Fraaije, G. Carrea, Biocatalytic properties of Baeyer–Villiger monooxygenases in aqueous–organic media, J. Mol. Catal. B Enzym. 39 (2006) 91–97.

[34] O.A. Stasyuk, H. Szatylowicz, C.F. Guerra, T.M. Krygowski, Theoretical study of electron-attracting ability of the nitro group: Classical and reverse substituent effects, Struct. Chem. 26 (2015) 905–913.

[35] D.E. Kim, C.D. ylan, B. David, Protein structure prediction and analysis using the Robetta server, Nucleic Acids Res. 32 (2004) 526–531.

[36] J. Pontius, J. Richelle, S.J. Wodak, Deviations from standard atomic volumes as a quality measure for protein crystal structures, J. Mol. Biol. 264 (1996) 121–136.